Experimental Evidence of Superposition and Superimposition of Cerebral Activity Within Pairs of Human Brains Separated by 6,000 Km: Central Role of the Parahippocampal Regions

Nicolas Rouleau, Lucas W. E. Tessaro, Kevin S. Saroka, Mandy A. Scott, Brendan S. Lehman, Lyndon M. Juden-Kelly and Michael A. Persinger

ABSTRACT

Previous experiments with chemiluminescent reactions indicated that when two loci separated by "non-local" distances shared specific temporal parameters of rotating magnetic fields with changing angular velocities the photon emissions doubled as if the spaces were superimposed. This excess correlation was considered an experimental demonstration of macroscopic entanglement. In the present study standardized LORETA (Low Resolution Electromagnetic Tomography) was employed to identify the location within pairs of human brains separated by approximately 6,000 km but who shared the same magnetic field parameters known to produce manifestations of entanglement. We predicted that when the frequency increment-dependent current densities within the cerebral volumes of the pairs during the entanglement condition were subtracted the regions with the minimum difference would simulate this superimposition. This superimposition occurred primarily for the theta band (4-8 Hz) within the parahippocampal regions, particularly within the right hemisphere, but only during the effector component of the exposure procedure when "entanglement" has been shown to occur. The results are consistent with the observations for photon emissions and shifts in the pH of spring water that demonstrated the properties of excess correlation between two loci. They exhibited the superposition of entanglement and the superimposition of space when a specific sequence of changing angular velocities circularly rotating magnetic fields was shared despite the non-locality.

Key Words: LORETA (Low Resolution Electromagnetic Tomography), parahippocampal region, entanglement, excess correlation, theta-activity, rotating magnetic fields, toroids, Arduino

DOI Number: 10.14704/nq.2015.13.4.891 **NeuroQuantology 2015; 4: 397-407**

Introduction

One of the primary consequences of approaching consciousness and the relationships between energy and matter from a *NeuroQuantology* perspective is that non-locality can be a central component to any process. Excess correlations between the responses of two discrete quantities or aggregates of energy, such as photons or molecules, have been demonstrated over distances of several tens of meters (Jin *et al.,* 2010) when random processes should dominate and the dissipation of propagation forces through the medium cannot accommodate the non-random relationship. The effect has been attributed to entanglement and occurs when a quantum system contains more than one particle such that the superposition principle elicits

Corresponding author: Dr. M. A. Persinger
Address: Consciousness and Neuroquantology Laboratory, Behavioural Neuroscience and Biomolecular Sciences Program, Laurentian University, Sudbury, Ontario, Canada P3E 2C6
e-mail ✉ mpersinger@laurentina.ca; ny_rouleau@laurentian.ca
Relevant conflicts of interest/financial disclosures: The authors declare that the research was conducted in the absence of any commercial or financial relationships that could be construed as a potential conflict of interest.
Received: Nov 8, 2015; **Accepted:** Nov 30, 2015

consistent excess correlation (Aczel, 2002). Most classic examples of entanglement involve photons or specific gases. In the present experiments we expanded a procedure that has produced reliable and conspicuous excess correlation between non-local volumes of chemiluminescent reactions (Dotta and Persinger, 2012) and shifts in parity in pH of spring water (Dotta *et al.,* 2013). We demonstrate that the current densities associated with quantitative electroencephalographic activities within human cerebrums separated by the Atlantic Ocean behave as if they were superimposed or occupied the "same space" only if the two brains shared the same circumcerebral, circular magnetic fields during the "entanglement" phase of the procedure.

Classical entanglement has been based primarily upon the responses of pairs or groups of pairs of photons although recent experiments have explored larger aggregates (Tura *et al.,* 2014). Evidence of experimentally induced entanglement for a protracted period within gas molecules has been reported by Julsgaard et al (2001). There is theoretical evidence and quantitative support that quantum energy "teleportation" may not be limited by distance (Hotta *et al.,* 2014) and that entanglement can occur between photons that have never co-existed (Megidish *et al.,* 2013) such as during the pre-contemporary state of the universe (Hu and Wu, 2006a,b). All of these models and approaches do not involve experimental conditions that could enhance entanglement beyond background or "natural" conditions.

Inspired by the concept of Tu et al (2005) that a photon could exhibit non-zero rest masses with a quantifiable upper boundary if the group and phase velocities differed, Dotta and Persinger (2012) exposed two small volumes of aqueous hypochlorite solutions to the same sequence of temporally patterned magnetic fields. The two containers were separated by 10 m. Each had been placed within a circular array of eight solenoids within which the rate of change in the production of the magnetic field and the phase or frequency modulation of the propagated pattern could be programmed by computer software. They found that if there were simultaneous injections of small amounts of hydrogen peroxide into the 10 m-separated solutions, there was a "doubling" of photon flux densities. In other words, the photomultiplier tubes measured twice the photon flux density than would be expected by random processes. It was as if the two spaces had been superimposed and hence "twice" the amount of reactant had been injected. However, this was evident only if a specific combination of accelerating group/decelerating phase and decelerating group/accelerating phase velocities were applied. This "entanglement" and excess correlation was evident for about 8 minutes after which it dissipated even though the fields were maintained and the injections continued.

There is a rich literature concerning macroscopic examples of non-locality. Korotaev et al (2005) described several examples of macroscopic non-locality or large-scale natural dissipative processes such as geomagnetic variation. Korotaev et al (2006) suggested that nonlocality within macroscopic systems does not appear to involve local carriers of interaction and information. These authors indicated that the entanglement occurs in space-time and hence there is the potential for forecasting solar and geomagnetic activity. That geomagnetic activity or small shifts in the intensity of the geomagnetic field adjacent to cells (Persinger *et al.,* 2015) and the human brain (Hunter *et al.,* 2010; Persinger *et al.,* 2013) are related have been shown experimentally. In general, for every 1 nT decrease in the static geomagnetic field within 15 cm from the person's right hemisphere there is an increase of $\sim 10^{-12}$ $W \cdot m^{-2}$ in photon flux density. The latter increases and decreases systematically with imagining white light and related cognitive states in comparison with mundane thoughts (Dotta *et al.,* 2012).

Evidence of "sudden information" accessed between two people with similar histories (Gurney *et al.,* 1886) separated by non-traditional distances (hundreds of kilometers) has been considered an example of excess correlation involving non-locality that could be a macro-manifestation of entanglement. The logical positivist's or behaviorist's definition of these phenomena, as suggested by Persinger (1974), is they are associations between stimuli and responses (or two non-local spaces) over marked discrepancies in space-time by mechanisms not known to date. The famous Duane and Behrendt (1965) experiment revealed excess correlation in the emergence of alpha activity when one of two separated twins was stimulated in about 10% of the cases. The remarkable experiments by Standish et al (2003; 2004) demonstrated a similar concordance for pairs of people if they

shared similar measurements during exposures to intense magnetic fields. Later, Persinger and his colleagues (2003; 2008) demonstrated that weak (microTesla) level magnetic fields employing the same equipment – that was later applied by Dotta and Persinger (2012) to the chemiluminescent experiments – produced evidence of excess correlation in the subjective experiences and reports of pairs of people who exhibited shared reinforcement histories when exposed to these fields.

Recently, Scott et al (2015) designed an experimental procedure employing an easily constructed technology that could simulate the more complex and expensive equipment employed in previous demonstrations. They found clear shifts in power spectral densities within the 7 Hz and 40 Hz bands in various regions of the brains of pairs of people who shared the same circumcerebral patterns of magnetic fields even when separated by the Atlantic Ocean but only during the "effector" or entanglement phase of the procedure. The other (primer) magnetic field conditions did not produce these effects. We reasoned that if the superposition associated with entanglement and the superimposition indicated by Dotta and Persinger's (2012) photon doubling experiment were applicable, then it should be evident within the volume of the brains of the participants as inferred by LORETA (Low Resolution Electromagnetic Tomography). Subtraction of the three-dimensional imaging of the pairs should indicate an absence of difference during the entanglement phase of the shared circular magnetic field exposures even though the two were separated by more than 6,000 km. The absence of difference in specific volumes of the cerebrums would be consistent with the superposition of space, or to employ a metaphor, the transposition of two brains into "one brain".

Materials & Methods

The precise details of the background of the five pairs of subjects, the details of the technology, and the schedules of presentation have been published previously by Scott et al (2015).

Toroid & Arduino

A toroid-shaped coil was placed over the head of each participant. Coupled to independent microcontrollers, the devices were set to pulse synchronized electromagnetic fields with counter-clockwise current flow. This configuration of paired-spaces was previously associated with reliable stimulus-response patterns as inferred by QEEG measures and sLORETA tomographs in task-naïve human participants who were not themselves directly exposed to the stimulus, but instead paired to an individual who was directly stimulated in real-time (Burke et al., 2013). Further experiments demonstrated that beakers of spring water that were paired using this technology displayed reliable shifts in pH with opposite direction in response to an injection of a weak acid within one of the beakers (Rouleau et al 2014). The distances involved in each experiment were 300 km and 1 m respectively, suggesting the effects were not influenced by the linear geographical distance between the spaces.

Figure 1. The custom-built toroid coil which generated the electromagnetic field patterns.

Coils, with diameters and circumferences of 25.4 cm and 79.8 cm respectively, consisted of plastic crotchet rings wrapped with 225 turns of 16 gauge insulated (stereo speaker) copper wire (Figure 1). Leads spliced to each end of a coil were connected to a solderless breadboard which was coupled to an Arduino Uno R3 microcontroller (Figure 2). Schematic representations of the board and microcontroller as seen in Figure 2 as well as a thorough analysis of the electromagnetic field effects associated with the device have been outlined by Rouleau & Persinger (2015).

Electromagnetic field patterns were synchronously generated within the spaces by

pulsed current flow as regulated by the microcontrollers. Two patterns, presented in sequence, were looped continuously during their respective presentation periods. The first pattern, the Primer, consisted of 7 all-or-none pulses, each with a rise-fall event consisting of 3 ms (Persinger and Koren, 2007). The time between the first and second pulse was 20 ms, which increased by 2 ms for each successive pulse within the set (i.e. 20 ms, 22 ms, 24 ms, etc.). The second pattern, the Effector, was similar in all respects with the exception that the first and second pulses were separated in time by 20 ms with a decrease of 2 ms for each successive pulse (i.e. 20 ms, 18 ms, 16 ms, etc.). The field exposure procedure lasted 20 mins, with the looped Primer field generated for the first 360 s, immediately followed by 840 s of the looped Effector field pattern. Two-dimensional representations of the patterns are displayed in Figure 3.

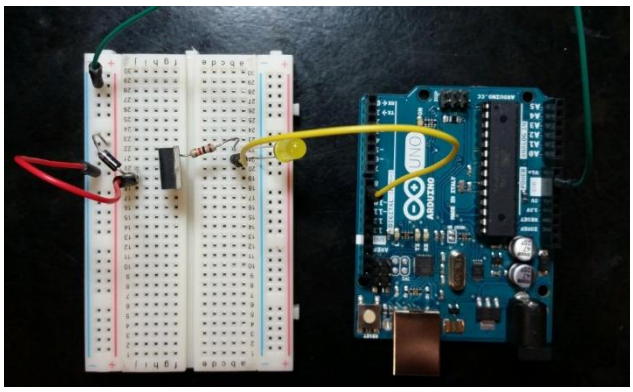

Figure 2. The custom circuit, coupled to an Arduino UNO R3 microcontroller.

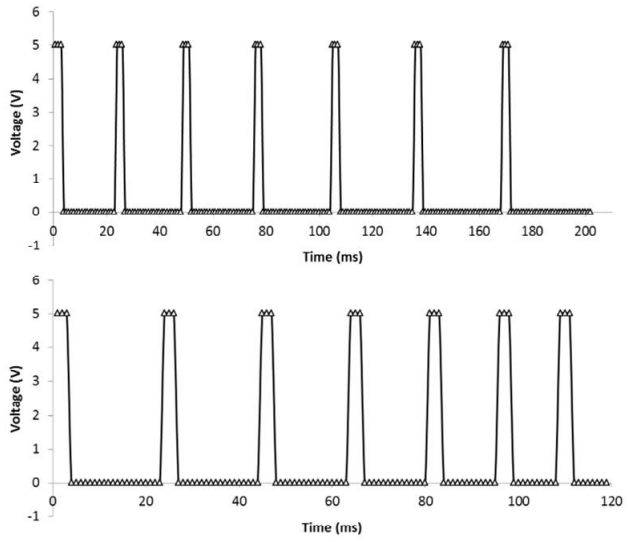

Figure 3. Two-dimensional representations of the Primer (top) and Effector (bottom) pulse patterns that were generated by the microcontrollers.

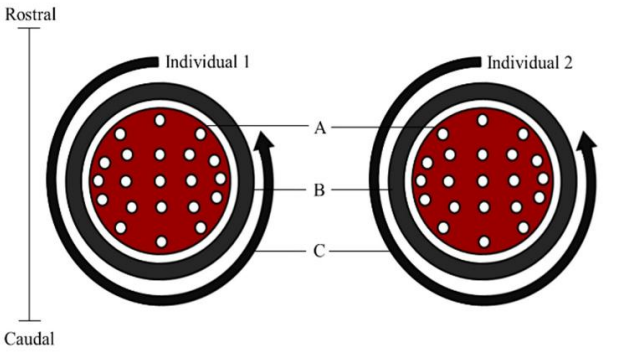

Figure 4. Aerial perspective of paired individuals, separated by >6000 km while wearing a QEEG cap (A) and toroidal coil (B). The direction of current flow through the coil (C) is also displayed.

Exposure Procedures

Once the QEEG caps were applied, and the toroids were placed over the heads of each participant (Figure 4), the paired-session was initiated. The participants first sat comfortably without any field exposure so that baseline electroencephalographic data could be collected. Pre-synchronized time keeping devices signaled the initiation of the Primer field after 660 s had elapsed. This was accomplished by plugging in the USB cord which formed the connection between the microcontroller and the laptop computer. This first pattern (the Primer) was continuously displayed for 360 s. Following the Primer field, manual initiation of the Effector field was accomplished by uploading code to the microcontroller within the Arduino 1.0.6 interface. The Effector field pattern was displayed for 840 s, after which the USB cord was unplugged from the laptop computer. Baseline QEEG recordings continued subsequent to field termination.

sLORETA Regions of Interest (ROI) & Current Source Densities

Raw data collected from all pairs were imported into MATLAB for amalgamation into a single dataset. Consequently, data for each pair consisted of 38 channels that were, upon synchronization, artifact corrected with the use of EEGLab (Delorme and Makeig, 2004). These raw data were then saved and parsed into sections corresponding to the different conditions (i.e. eyes open, eyes closed, field application, etc.). The synchronized data were then separated into two separate EEG cases for

computation of parahippocampal current source density (μA/mm²) within the right (MNI coordinates: X=28, Y=-40, Z=-12) and left (X=-28, Y=-40, Z=-12) hemispheres completed within sLORETA (Pascual-Marquis, 2002) for each condition separately.

The approach considered here was similar to that used in a previously published study (Saroka et al., 2014). Consequently 2 (Person A or Person B) x 22 (conditions) computations were performed. First, the raw time-series data were transformed into the frequency-domain by cross-spectral coherence within the delta (1.5-4 Hz), theta (4-7 Hz), low-alpha (7-10 Hz), high-alpha (10-13 Hz), beta-1 (13-20 Hz), beta-2 (20-25 Hz), beta-3 (25-30 Hz) and gamma (>30 Hz) frequency bands using the EEG to Cross-spectrum function. These data were then translated onto a 3-D brain using a custom 19-channel transformation matrix for the computation of current source densities within each voxel using the *Cross-Spectrum to sLORETA* function. Finally, the ROI-specific seeds along with these translated data were entered into the sLOR to ROI function where regionally-specific estimations of current source density were extracted for the left and right parahippocampal gyri. The resulting estimates were then consolidated into a single database and exported into a text file for importation into SPSS.

sLORETA Tomographs

All data were handled in ASCII format. Artifact-removed and temporally synced raw quantitative electroencephalography (QEEG) data underwent standardization (Z-score conversion) to remove any effects of the recording devices and emphasizing differences between the subjects' brain activity using MatLAB 2014b software. The standardized data for each condition were then segmented into five chunks of 2500 points, or five segments of 10 sec of EEG data within MatLAB. The EEG data were then converted to standardized low-resolution brain electromagnetic tomography analysis (sLORETA) files (.slor) using version 2015-04-15 of the LORETA software.

sLORETA is a functional imaging method based on electrophysiological data, in this case QEEG. The algorithm of sLORETA takes into account related and neighboring neuronal structures and applies it to the neuroanatomical constraints of the digitized Montreal Neurological Institute (MNI) coordinate system and represents the cortex as volume elements (voxels). It has been demonstrated to be an efficient tool for functional brain mapping as indicated by comprehensive experimental validation of its localization accuracy.

The conversion from ASCII to .slor files incorporates a specification of the 19-electrode coordinates and a transformation matrix. The conversion employs cross-spectrum analyses within the eight classical frequency bands – delta (1.5-6 Hz), theta (6.5-8 Hz), low-alpha (8.5-10 Hz), high-alpha (10.5-12 Hz), beta-1 (12.5-18 Hz), beta-2 (18.5-21 Hz), beta-3 (21.5-30 Hz) and gamma (>30 Hz). The analytical design employed within the sLORETA software investigated differences between respective pairs of subjects during the six rest/tone conditions of the exposure paradigm.

Thus, the five .slor files for a subject in a pair during each rest/tone condition were compared to their counterpart's five .slor files during the same condition. For each comparison, one single test (Log of ratio of averages) was calculated for all five-segment pairs for each analysis with 5000 random permutations (or bootstrapping). Statistical significance levels were corrected for multiple comparisons. The resulting tomographs, comprised of 6,239 voxels with 5 mm resolutions, highlighted those regions that showed the greatest difference in activity based on Brodmann designations in MNI space.

Results

Normal and Expected Patterns

The validity and limitations of any measurement tool and method can be estimated by discerning its congruence with respect to what is already known or established within the field of inquiry. One of the most well-known and historical phenomenon associated with cognitive cerebral activity is the enhanced power within the alpha range when the eyes are closed compared to when they are opened. As shown in Figure 5, when the eyes were closed the current densities were increased (areas of yellow higher than reddish hues) within the caudal portion of the hemispheres and included the parietal, caudal temporal and occipital lobes. This classical and conspicuous enhancement is seen within (from left to right) the horizontal, mid-sagittal and

coronal section. The specific portions of the three axes of these sections reflect the position at which the effect was maximal. The cm designations refer to the distance (in cm) within the cerebrum for each plane with respect to the origin which is the level of the anterior commissure.

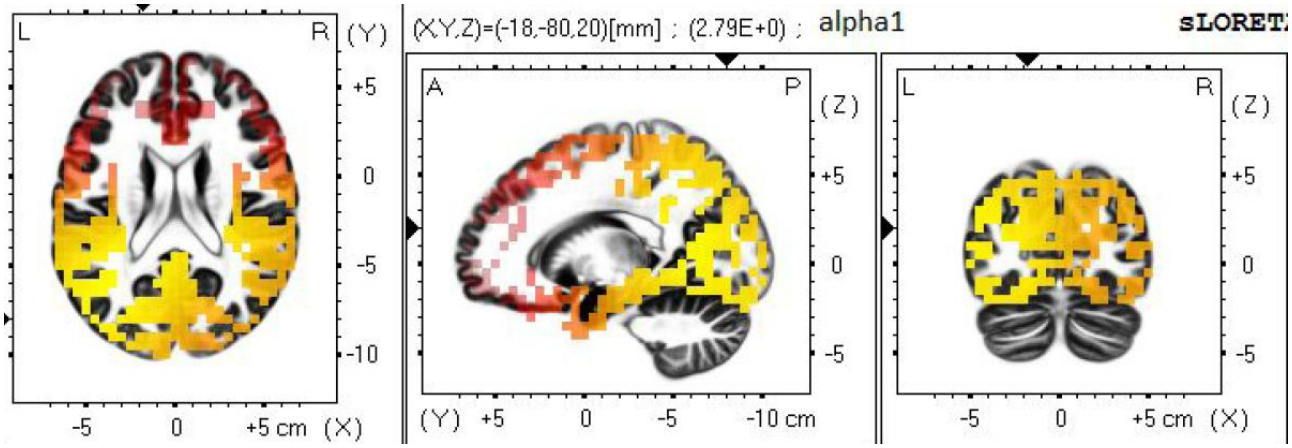

Figure 5. Net enhancement of electric current density within the areas indicated by yellow within at the peak sections for the horizontal, sagittal and coronal positions when the eyes were closed compared to when they were opened.

Figure 6 is a composite of all 10 participants during times while consciously intending or cognitively focusing to "send" or "receive" information. The current densities increased within the beta-2 band and were focused within the left prefrontal regions as indicated by the yellow color. This is evident for the horizontal section as well as the lateral sagittal, and very rostral coronal levels. The light reddish color indicates activation (increased current densities) but to a lesser degree within the left hemisphere within the regions that would include the temporal-frontal connections. This would be approximately the initiation and termination of the superior longitudinal (arcuate) fasciculus. This activation was not observed in the right hemisphere.

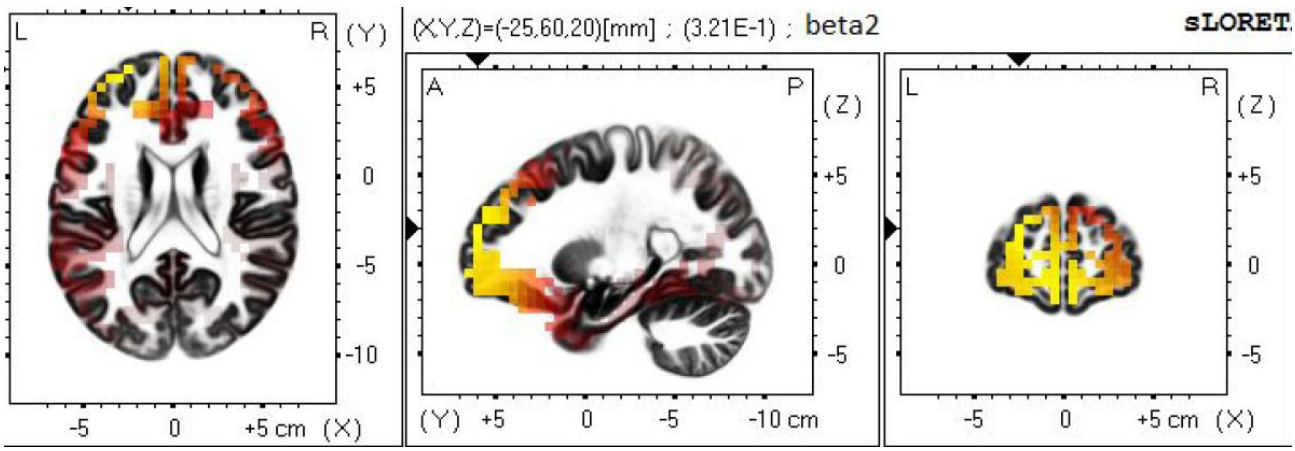

Figure 6. Averaged (for the 10 participants) net increase in current density (indicated by yellowish color) within the left frontal region during periods of "intending" to send or receive information. Reddish color indicates similar but less intense activation. Note the predominance of the left hemisphere only for the involvement of the temporal lobe.

Possible Excess Correlation (Entanglement) Indicators

If the LORETA demonstrates such classic functions as eyes opened/closed differences in alpha power within the caudal hemisphere and high beta activity differences within the left prefrontal region during intention and concentration, then even subtle changes should

be evident. In the present experiment these subtle differences involved the superposition effects only during the entanglement portion of the experiment. The quintessential test of the superposition and superimposition effect when two cerebrums, exposed to the same circumcerebral magnetic fields with specific changing angular velocities, converge into the "same space" is the absence of random individual differences within shared loci of both brains even though they were separated by more than 6,000 km. When all of the bands of QEEG activity were carefully assessed the only conspicuous and reliable evidence of superposition occurred within the *theta* band (4-8 Hz).

The effect is evident in Figure 7. The areas to consider are the ones indicated by the red arrow designated in the horizontal section of the brain indicated in the grey reference diagrams to the right. This is the general area of the parahippocampal gyrus and the hippocampal formation within that area. The five rows reflect the five pairs each member of which was separated by the >6,000 km distance. Each horizontal section reflects the *differences* in current density as inferred by LORETA within the theta (4-8 Hz) band between the two members of each pair. The condition to which both members of the pair were exposed simultaneously is shown in the columns. They were Pre (pre-magnetic field stimulation), Pri1 (the first part of the Primer field, Pri2 (the second part of the primer field), Eff1 (the first part of the Effector field), Eff2 (the second part of the Effector field), and Pos (post baseline).

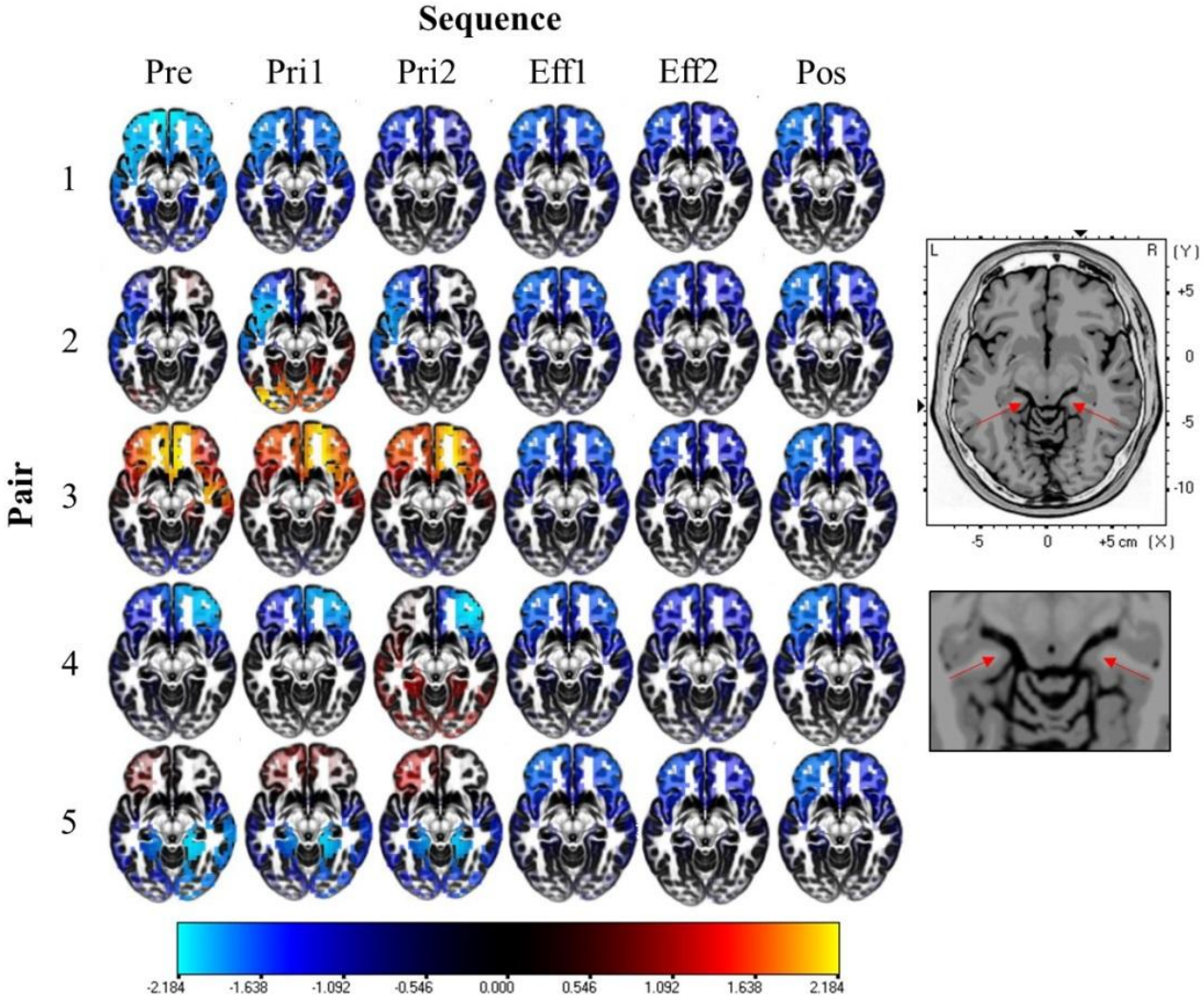

Figure 7. Theta-band (6.5 Hz – 8 Hz) current source densities within MNI space displaying generalized decreases in parahippocampal differences between paired individuals which was initiated during the Effector 1 (Eff1) sequence which persists throughout Effector 2 (Eff 2) and Post-Exposure (Pos) sequences.

The presence of color in any of the sections indicates a discrepancy in current densities within the theta band between the two members of the pair. Statistically significant differences were indicated by blue and yellow gradations. Even within these figures the presence of discrepancies during the baseline (pre) and the two Primer field conditions are evident. The discrepancies are not as evident in every pair because of the limits of the color coding. However quantitatively they were clearly evident for all five pairs. The differences had been obtained by subtracting the LORETA data from the person in Europe from the LORETA data from the person in Sudbury. The blue indicates that the current densities for the people in Sudbury were less than those densities for people in Europe for all of the pairs except pair 3. In this instance the Sudbury member of the pair exhibited more current density within those regions.

Once the Effector fields began (Eff1, Eff2) there was a marked homogeneity of differences between the members of all 5 pairs that was remarkably similar. Even though the color patterns within the horizontal sections for all 5 pairs looks similar (as if they are simply replicates of the same image) detailed analyses of the pixels indicated that different patterns of discernable pixels occurred in each of the separate pair differences. They are simply not discernable at the resolution depicted in Figure 7. The consistency of this effect was verified by a second experimenter who analyzed the data independently.

However, the actual test of the superposition and superimposition manifestation is the absence of differences that occurred for all 5 pairs within the parahippocampal regions. Close inspection of the pixels (125 mm^3 or 5 x 5 x 5 mm pixels) in the images indicated minimal discrepancies between each of the two brains during Eff1 and Eff2. The effect continued into the post-baseline period when no field was present.

Although the hemispheric differences are not discernable from Figure 7, quantitative analyses of the pixel values clearly showed statistically significant correlations between the values within the parahippocampal gyri for the pairs of participants. As shown in Figure 8, the right parahippocampal theta power ($\mu V^2 \cdot Hz^{-1}$) displayed a significant positive correlation between paired-participants during the first half of the Effector sequence, rho = .71, p<.001 (Figure 1). Similarly, left parahippocampal theta power displayed a significant positive correlation between paired-participants during the second half of the Effector sequence, rho = .45, p<.05. The duration of each half was 6 min.

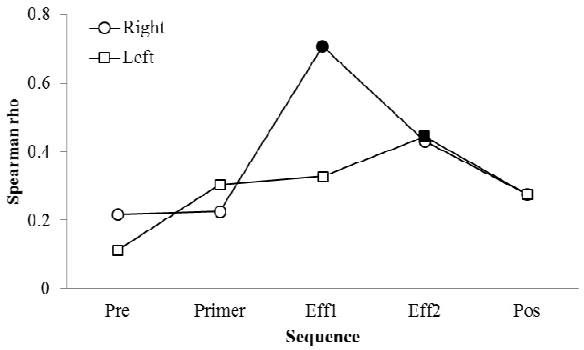

Figure 8. Strength of the association of inferred theta power of paired right (circles) and left (squares) parahippocampal gyri over sequences of the experiment. Closed symbols indicated statistically significant coefficients.

There were conspicuous absences of statistically significant correlations and association that are equally important. First, the inter-pair correlations within the theta range were not statistically significant during the Primer fields (1 and 2 combined for simplicity) and the post-baseline condition. The strengths of these coefficients did not differ appreciably from the pre-baseline condition before any fields were presented. The absence of statistically significant correlations for the Primer fields for the theta power within the shared parahippocampal regions strongly indicates the significant associations during the Effector phases were not simple artifacts of shared proximal fields. The primary manifestation within the theta band rather than a diffuse enhancement across all bands and the delay of the effect for the right and left parahippocampal regions specifically (rather than large cerebral volumes) also supports the conclusion that the effect was not likely to be artifact from independent local effects but rather an excess correlation.

Discussion

The results of this study confirm the extensive QEEG and spectral power density analyses by Scott et al (2015). They showed that when two people share the same circularly generating magnetic fields composed of 3 ms point durations and delivered with a specific sequence of changes

in angular velocity excess correlations within the same brain spaces occurred even though they were separated by more than 6,000 km. We were careful to ensure that potential artifacts or the effects from potential artifacts were minimized as much as possible. Because both members of each pair were exposed to the same magnetic field sequences one could argue that any similarity between the two participants only reflects the responses to the local magnetic fields. The two people show similarity simply because they are responding to the same local stimulus. For example, two people separated by large distances might both look at their respective clocks at the same time and experience the cerebral representations of the same configurations. However, that does not indicate that both share the experience because of non-locality.

However if the consistency of the diminished individual differences in the pairs specifically within the theta band only during the Effector phase and manifested within only the parahippocampal regions were due to independently induced artifact (like the two people separated by great distances looking at separate clocks with the same time), then one would expect comparable increased current densities for both the Primer and Effector fields because both involved the same intensity and point durations but only differed by the slight difference in angular velocities. The results clearly indicated that the absence of differences between the pairs of cerebral current densities only occurred during Effector phase. This is the same effect we have observed with this paradigm for photon reactions and shifts in pH separated by non-local distances when they shared rotating magnetic fields generated within a circular array of solenoids or through toroids with the same temporal patterns.

Non-specific effects are not likely from the simple application of the toroidal fields because only the theta band was affected. This is the band that both our theory (Buzsaki, 2002) and the most common correlate for spontaneous cases of remote viewing (Persinger *et al.,* 2002) would predict. In general, one would not expect current shifts associated with such a narrow band from either induction or resonant interactions from applied fields. Although the intrinsic resonance for the grey matter based upon direct measurements of capacitance and inductance at 1 kHz (the duration of an action potential) does solve to be around 7 Hz (Persinger *et al.,* 2008), there would be no obvious mechanism by which the low intensities (30 mG; $3 \cdot 10^{-8}$ T) and estimated rotational velocities from the Arduino-based shifts in point durations moving through the toroid (which would be within the kHz range) would focus only within the theta band. One would expect more diffuse involvement of most of the frequency bands.

The locality of the effects within the five pairs of cerebrums also minimizes the likelihood that local artifacts were involved. The evidence of superimposition of loci occurred within the parahippocampal regions and not within other areas. Although one could argue that the parahippocampal region is sensitive to applied weak magnetic fields, this would not easily accommodate the initial responsiveness of the right hemisphere during the first 6 min of the Effector phase only followed by the enhanced responsiveness of the left hemisphere during the second 6 min of the Effector phase. Such differential response latencies are not typical of induced artifacts. Consequently, in the balance of probabilities the most parsimonious explanation for the consistent and specific effects that would meet the criteria for excess correlation and entanglement is that the results are evidence of this effect.

The mechanisms and processes by which this entanglement occurred would be expected to follow known energetic relationships and physical principles. The intensity of the changing angular velocity magnetic fields was about 30 mG ($3 \cdot 10^{-8}$ T). The direction of the current around the toroid was counterclockwise and the direction of the magnetic field would have been perpendicular to the horizontal plane of the subjects' heads. This means the direction of the magnetic field (B) would have been dorsal-to-ventral or slightly deviated from the axis from the brain stem to the cerebral cortices. The B vector would have been repeatedly reversing direction between towards the ionosphere and towards the ground.

According to traditional estimates of energy from magnetic fields within a volume, the change in energy from the $3 \cdot 10^{-8}$ T fields can be calculated by:

$$E = B^2 (2\mu)^{-1} \cdot m^3 \quad (1),$$

where B is the strength of the field, μ is magnetic susceptibility ($4\pi \cdot 10^{-7}$ $N \cdot A^{-2}$) and m^3 is volume.

For the entire cerebrum of 10^{-3} m^3, the averaged energy would be $\sim 7 \cdot 10^{-13}$ J per second of renewal. Because each action potential is associated with $\sim 2 \cdot 10^{-20}$ J (Persinger, 2015; 2012; 2010), this would be equivalent to $3.5 \cdot 10^{7}$ action potentials. If each neuron were discharging within the theta band, this would be equivalent to between 1 million to 10 million neurons. This range has been associated with the critical number associated with a "percept" or experience (Rouleau and Dotta, 2014), and, is equivalent to the numbers of primary neurons within the human hippocampal formation (Gloor, 1997).

When Marconi first generated experimentally small electromagnetic pulses across the Atlantic he had to accommodate the compatibility between his source of generation and the properties of wave space. For excess correlations between complimentary shifts in pH within two volumes of water separated by non-local distances the optimal frequency of the angular rotation was balanced with that obtained from the product of the magnetic moment of the proton and the intensity of the magnetic field divided by Planck's constant. When this occured the magnitude of the shift attributed to excess correlation increased by almost a factor of 10. This is much slower than the potential frequency inferred from the duration of the Primer (128 ms) and Effector (203 ms) fields. The time for an electrical signal to traverse the linear distance of the wire within the toroid coil, would require about 50 ns.

The toroid system is quite different from the circular array of solenoids employed in previous experiments. It may involve different mechanisms. The most conspicuous feature of this system is the 1 to 5 nT attenuation of the earth's local static magnetic field during the production of the fields in the east-west direction. If these values were applied to the relationship between frequency and the product of the field strength and proton magnetic moment divided by Planck's constant, the frequency is even less but conceptually significant. The frequency equivalence ranges between 0.021 Hz (47 s) to .106 Hz (9 s). The mass equivalences of energy values ($1.4 \cdot 10^{-35}$ J to $7 \cdot 10^{-35}$ J) range between $1.5 \cdot 10^{-52}$ kg to about $7 \cdot 10^{-52}$ kg. The former is the upper boundary for the rest mass of a photon (Tu *et al.,* 2005). Although there are clearly other explanations the orthogonal directions of the attenuated static field and the dynamic toroid field could create the conditions for the type of photon involvement (Vaziri *et al.,* 2002) derived from the Lorentz Lemma that would allow superimposition with the Schumann Resonances (Nickolaenko and Hayakawa, 2014) that occupy the space between the earth's surface and the ionosphere and most if not all human brains (Persinger and Saroka, 2015; Saroka and Persinger, 2014).

References

Aczel AD. Entanglement: the greatest mystery in physics. Raincoast: Vancouver, 2002.

Burke RC, Gauthier MY, Rouleau N & Persinger MA. Experimental demonstration of potential entanglement of brain activity over 300 km for pairs of subjects sharing the same circular rotating, angular accelerating Magnetic fields: verification by s_LORETA, QEEG measurements. Journal of Consciousness Exploration & Research 2013; 4(1).

Buzsaki G. Theta oscillations in the hippocampus. Neuron 2002; 33: 325-340.

Delorme A & Makeig S. EEGLAB: an open source toolbox for analysis of single- trial EEG dynamics including independent component analysis, Journal of Neuroscience Methods 2004; 134: 9–21.

Dotta BT and Persinger MA. Doubling of local photon emissions when two simultaneous, spatially separated chemilumiescent reactions share the same magnetic field configurations. Journal of Biophysical Chemistry 2012; 3: 72-80.

Dotta BT, Murugan NJ, Karbowski LM and Persinger MA. Excessive correlated shifts in pH within distal solutions sharing phase-uncoupled angular accelerating magnetic fields: macro-entanglement and information transfer. International Journal of Physical Sciences 2013; 8:1783-1787.

Dotta BT, Saroka KS and Persinger MA. Increased photon emission from the head while imaging light in the dark is correlated with changes in electroencephalographic power: Support for Bokkon's biophoton hypothesis. Neuroscience Letters 2012; 513: 151-154.

Duane TD & Behrendt T. Extrasensory electroencephalographic induction between identical twins. Science 1965; 150: 367.

Gloor P. The temporal lobe and limbic system. New York, NY: Oxford University Press, 1997.

Gurney E, Myers FWH and Podmore F. Phantasms of the living. Truebner: London, 1886.

Hotta M, Matsumoto J and Yusa G. Quantum energy teleportation without a limit of distance. Physical Review A 2014; 89: 012311.

Hotta M, Matsumoto J and Yusa G. Quantum energy teleportation without limit of distance. Physical Review A 2006; 89: 012311.

Hu H and Wu M. The essence and implications of quantum entanglement and the story of spin-mediated consciousness theory. NeuroQuantology 2006a; 1: 5-16.

Hu H and Wu M. Thinking outside the box II: The origin, implications and applications of gravity and its role in consciousness. NeuroQuantology 2006b; 4 : 291-306.

Hunter MD, Mulligan BP, Dotta BT, Saroka KS, Lavalle CF, Koren SA and Persinger MA. Cerebral dynamics and discrete energy changes in the personal physical environment during intuitive-like states and perceptions. Journal of Consciousness Exploration & Research 2010; 1: 1179-1197.

Jin X-M, Ren J-G, Yang B, Yi Z-H, Zhou F., et al. Experimental free-space quantum teleportation. Nature photonics 2010; DOI: 10.1038, Nphoton.2010.87.

Julsgaard B, Kozheikin A and Polzik ES. Experimental long-lived entanglement of two macroscopic objects. Nature 2001; 413: 400-403.

Korotaev SM, Morozov AN, Serdyuk VO, Gorohov JV and Machinin VA. Experimental study of macroscopic nonlocality of large-scale natural dissipative processes. NeuroQuantology 2005; 3(4): 275-294.

Korotaev SM, Serdyuk VO and Gorohov JV. Forecast of solar and geomagnetic activity on the macroscopic nonlocality effect. Hadronic Journal 2006; 29: 679-696.

Nickolaenko A and Hayakawa M. Schumann Resonance for Tyros. Springer, Tokyo, 2014.

Pasqual-Marquis RD. Standardized low resolution brain electromagnetic tomography (sLORETA): Technical details, Methods and Findings in Experimental Pharmacology 2002; 24: D5–D12.

Persinger MA and Koren SA. A theory of neurophysics and quantum neuroscience: implications for brain function and the limits of consciousness. International Journal of Neuroscience 2007; 117: 157-175.

Persinger MA and Saroka KS. Human quantitative electroencephalographic and Schumann Resonance exhibit real-time coherence of spectral power densities: implications for interactive information processing. Journal of Signal and Information Processing 2015; 6: 153-164.

Persinger MA, Dotta BT, Karbowski LM and Murugan NJ. Inverse relationship between photon flux densities and geomagnetic intensities over cell aggregates: quantitative evidence for energetic conservation. FEBS OpenBio 2015; 5: 413-418.

Persinger MA, Dotta BT, Saroka KS and Scott MA. Congruence of energies for cerebral photon emissions, quantitative EEG activities and 5 nT changes in proximal geomagnetic field support spin-based hypothesis of consciousness. Journal of Consciousness Exploration & Research 2013; 4: 1-24.

Persinger MA, Koren SA and Tsang EW. Enhanced power within a specific band of theta activity in one person while another receives circumcerebral pulsed magnetic fields: a mechanism of influence at a distance? Perceptual and Motor Skills 2003; 97: 877-894.

Persinger MA, Roll WG, Tiller SG, Koren SA and Cook CM. Remote viewing with the artist Ingo Swann: Neuropsychological profile, electroencephalographic correlates, magnetic resonance imaging (MRI) and possible mechanisms. Perceptual and Motor Skills 2002; 94: 927-949.

Persinger MA, Tsang EW, Booth N and Koren SA. Enhanced power within a predicted narrow band of theta activity during stimulation of another by circumcerebral weak magnetic fields after weekly spatial proximity: evidence for macroscopic quantum entanglement? NeuroQuantology 2008; 6: 7-21.

Persinger MA. 10^{-20} Joules as a neuromolecular quantum in medicinal chemistry: an alternative approach to myriad molecular pathways. Current Medicinal Chemistry 2010; 17: 3094-3098.

Persinger MA. Brain electromagnetic activity and lightning: potentially congruent scale-invariant quantitative properties. Frontiers in Integrative Neuroscience 2012; 6, article 19.

Persinger MA. The paranormal: the patterns and mechanisms (2 volumes). M.S.S. Information. N.Y., 1974.

Persinger MA. Thixtotropic phenomena in water: quantitative indicators of Casimir-magnetic field transformations from vacuum oscillations (virtual particles). Entropy 2015; 17: 6200-6212.

Rouleau N & Persinger M. Local electromagnetic fields exhibit temporally non-linear, east-west oriented 1-5 nT diminishments within a toroid: empirical measurement and quantitative solutions indicating a potential mechanism for excess correlation. Journal of Electromagnetic Analysis and Applications 2015; 7: 19-30.

Rouleau N and Dotta BT. Electromagnetic fields as structure-function zeitgebers in biological systems: environmental orchestration of morphogenesis and consciousness. Frontiers in Integrative Neurosciences 2014; 8:84. doi: 10.3389/fnint.2014.00084

Rouleau N, Carniello TN & Persinger MA. Non-local pH shifts and shared changing angular velocity magnetic fields: Discrete energies and the importance of point durations. Journal of Biophysical Chemistry 2014; 5: 44-53.

Saroka KS and Persinger MA. Quantitative evidence for direct effects between earth-ionosphere Schumann Resonances and human cerebral cortical activity. International Letters of Chemistry, Physics and Astronomy 2014; 20: 166-194.

Saroka KS, Caswell JM, Lapointe A & Persinger MA. Greater electroencephalographic coherence between left and right temporal lobe structures during increased geomagnetic activity. Neuroscience Letters 2014; 560: 125-130.

Scott MA, Rouleau N, Lehman BS, Tessaro LWE, Juden-Kelly LM, Saorka KS and Persinger MA. Experimental production of excess correlation across the Atlantic Ocean of right hemispheric theta-gamma power between subject pairs sharing circumcererbal rotating magnetic fields. Journal of Consciousness Research & Exploration 2015; 6: 658-707.

Standish LA, Johnson LC, Richards T & Kozak L. Evidence of correlated functional MRI signals between distant human brains. Alternative Therapy and Health Medicine 2003; 9: 122-128.

Standish LA, Kozak L, Johnson LC & Richards T. Electroencephalographic evidence of correlated event-related signals between brains of spatially and sensory isolated human subjects. The Journal of Alternative and Complementary Medicine 2004; 10: 307-314.

Tu L-C, Luo J and Gilles GT. The mass of the photon. Reports on Progress in Physics 2005; 8: 77-130.

Tura J, Augusiak R, Sainz AB, Vertesi T, Lewenstein M and Acin A. Detecting nonlocality in many-body quantum states. Science 2014; 344: 1256-1258.

Vaziri A, Weihs G and Zeilinger A. Experimental two-photon, three dimensional entanglement for quantum communication. Physical Review Letters 2002; 89: 230401.